

# Benchmark Experiment to Prove the Role of Projectile Excited States Upon the Ion Stopping in Plasmas

Y. T. Zhao<sup>1,2,\*</sup> Y. N. Zhang,<sup>1,3</sup> R. Cheng,<sup>2,†</sup> B. He<sup>3,‡</sup> C. L. Liu,<sup>3</sup> X. M. Zhou,<sup>1,4</sup> Y. Lei,<sup>2</sup> Y. Y. Wang,<sup>2</sup> J. R. Ren,<sup>1</sup> X. Wang,<sup>1</sup> Y. H. Chen,<sup>2</sup> G. Q. Xiao,<sup>2</sup> S. M. Savin<sup>5</sup>, R. Gavrilin,<sup>5</sup> A. A. Golubev<sup>5,6</sup> and D. H. H. Hoffmann<sup>1,6</sup>

<sup>1</sup>MOE Key Laboratory for Nonequilibrium Synthesis and Modulation of Condensed Matter, School of Science, Xian Jiaotong University, Xian 710049, China

<sup>2</sup>Institute of Modern Physics, Chinese Academy of Sciences, Lanzhou 730000, China

<sup>3</sup>Institute of Applied Physics and Computational Mathematics, Beijing 100088, China

<sup>4</sup>Xianyang Normal University, Xianyang 712000, China

<sup>5</sup>Alikhanov Institute for Theoretical and Experimental Physics (ITEP) of National Research Center “Kurchatov Institute,” Moscow 117218, Russia

<sup>6</sup>National Research Nuclear University MEPhI (Moscow Engineering Physics Institute), Moscow 115409, Russia



(Received 8 February 2020; revised 27 January 2021; accepted 16 February 2021; published 15 March 2021)

We report on a precision energy loss measurement and theoretical investigation of 100 keV/ $u$  helium ions in a hydrogen-discharge plasma. Collision processes of helium ions with protons, free electrons, and hydrogen atoms are ideally suited for benchmarking plasma stopping-power models. Energy loss results of our experiments are significantly higher than the predictions of traditional effective charge models. We obtained good agreement with our data by solving rate equations, where in addition to the ground state, also excited electronic configurations were considered for the projectile ions. Hence, we demonstrate that excited projectile states, resulting from collisions, leading to capture-, ionization-, and radiative-decay processes, play an important role in the stopping process in plasma.

DOI: [10.1103/PhysRevLett.126.115001](https://doi.org/10.1103/PhysRevLett.126.115001)

Ion stopping in plasma is a fundamental process and new, unreckoned phenomena were recently discovered with intense laser-generated particle beams [1]. Investigation of energy loss processes in solid or gaseous matter has been a very active research topic for decades. A large number of sophisticated theories and a rich experimental database exists. In deuterium-tritium fusion scenarios alpha particle stopping is the relevant heating mechanism, and a precise knowledge of the stopping power is of utmost importance to achieve propagating burn of the compressed fuel in inertial fusion targets [2–4]. The advent of plasma targets at accelerator facilities initiated a number of experimental activities to study beam plasma interaction phenomena with ionized matter [5–9]. Cayzac and co-workers [5] performed an experiment using a laser-generated plasma. Their data disproved several standard stopping-power models for low velocity ions near the Bragg-peak region, and supported those theoretical approaches that included a detailed treatment of strong ion-electron collisions. Numerous models are able to reproduce the experimental results for fully ionized plasma and high energy beams. However, the database for low energy ions propagating in partially ionized plasma is still limited, and commonly used theories [10–12] need to be benchmarked.

Among the problems, yet unsolved, is the influence of excited projectile states on the stopping process. Presently the dynamic evolution of the projectile electronic

configuration and its influence on the stopping process is widely ignored or taken into account by an effective charge ( $Z_{\text{eff}}$ ) [10,11]. The contribution of different charge states is averaged by this procedure, and the average projectile, characterized by  $Z_{\text{eff}}$ , is assumed to be in the ground state. Energy loss is predominantly due to collisions with electrons. Excited states are prevalent in beam plasma interaction processes, regardless of the projectile species and plasma state. Because of their reduced binding energy the ionization probability increases and a higher ionic charge state results with less shielding of the nuclear charge, and thus the energy loss is different from ions in a ground state [13].

The difference in charge state distribution and stopping power of solid and gas targets is a well-known fact, and was attributed to the high collision frequency in solid targets as compared to gas targets, which leads to highly excited projectile states. More than 30 years ago it was already pointed out that processes involving excited states lead to a substantial increase in the stopping cross section for a neutral beam injected into a tokamak plasma [14]. But there is little experimental evidence to precisely pin down the role of excited states. This requires a precision experiment and a simple well-defined collision system which we will describe here. In previous experiments with discharge plasma or laser-generated plasma, and highly charged heavy ions as projectiles, an effective charge state  $Z_{\text{eff}}$

was chosen to match simultaneously the measured energy loss and the charge state distribution data [15,16]. Nevertheless, these experiments did not reveal details on how excited projectile states do affect the charge state distribution and energy loss. In order to unambiguously demonstrate the role of excited states we choose the most-simple beam plasma configuration, alpha particles and hydrogen plasma, to study the ion stopping process in a situation that is accessible for both experiment and simulation, since only a limited number of excited states and transfer channels are involved.

The long interaction time, which corresponds to the plasma transit time of the beam, and close multiple collisions in the low energy regime poses also challenges for the theoretical modeling of the situation. Even though several models, including *ab initio* models, have been developed, it is still an intricate undertaking to describe the evolution of the projectile ionic state distribution. When Jacoby *et al.* [9] measured a 35 times higher energy loss for Kr ions in fully ionized hydrogen plasma as compared to cold hydrogen gas, this was attributed to a rise in charge state from  $1+$  up to  $6+$  while the Kr ion was traversing the plasma discharge. To the best of our knowledge, previous experiments did not reveal details on how projectile excited states do affect the charge state distribution, and in consequence the stopping process.

We performed a high-precision measurement of alpha particle stopping in a hydrogen-discharge plasma. The alpha particle energy was as low as  $100 \text{ keV/u}$ . The plasma lifetime of this experiment is in the  $\mu\text{s}$  range due to the characteristics of the discharge circuit. Compared to laser-generated plasma the gradients in plasma density and temperature are low in the beam-plasma interaction region and the plasma is stable compared to the transit time of the beam ions. This allows a high-precision comparison of experiment and theory.

The measurement was carried out at the 320 kV high-voltage platform of IMP, Lanzhou, using an electron cyclotron resonance ion source (ECRIS) to produce the  $\text{He}^{2+}$  ion beam with a current of about 100 nA. The entrance aperture of the plasma tube reduced the beam radius to 0.5 mm. The experimental configuration is shown in Fig. 1. A time-gated microchannel-plate (MCP) detector, positioned behind the  $45^\circ$  bending magnet, recorded the ions passing through the plasma. This setup permits an energy resolution of 1 keV. The discharge tube is made up of two quartz tubes of 78 mm in length, with the high-voltage electrode placed in the middle and the grounded electrodes at either end. A similar discharge plasma was used in an experiment many years ago [8,17]. The advantage of this configuration is twofold. First, in a linear discharge the discharge current produces an azimuthal magnetic field that acts as a plasma lens on the ion beam. Having the high-voltage electrode placed at the center the second part of the discharge tube cancels in zero order the

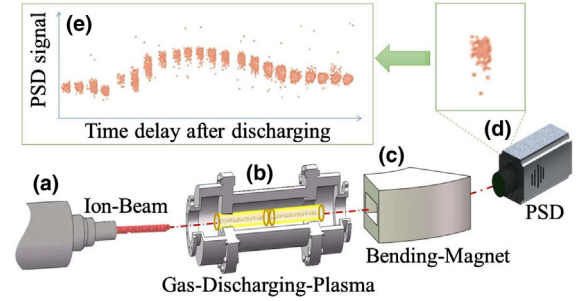


FIG. 1. Layout of the experiment. The  $\text{He}^{2+}$  ion beam from the accelerator (a) was collimated into a gas-discharging plasma (b) and bended by a magnet (c), then recorded by a fast-gated position sensitive detector (PSD) (d). By sorting the PSD signals in the sequence of the time delay after discharge (e), the temporal profile of energy loss was obtained.

plasma lens effect of the first part and thus ensures high transmission of the beam. Second is the safety effect, having the grounded parts of the discharge tube connected to the beam pipe. The vacuum of the beam pipe is maintained by differential pumping. While the initial gas pressure is varied between 1 and 5 mbar, the resulting hydrogen plasma during a discharge at 3 kV is at a temperature of 1–2 eV, and a free electron density of  $10^{16} - 10^{17} \text{ cm}^{-3}$ . At the peak time of 3 s the linear free electron density was determined to be  $4.48 \times 10^{17} \text{ cm}^{-2}$  with an ionization degree of 31%. The plasma parameters were diagnosed by Mach-Zehnder interferometry following the same procedures as outlined in Ref. [18]. Our calculations of energy loss are based on the interferometry parameters.

Prior to the alpha particle stopping experiment we measured the proton energy loss with the same setup and a proton initial energy of 100 keV. We varied the gas density and the discharge voltage in the same regime as in the main experiment. The proton measurements, since there is no charge state effect, showed excellent agreement with theoretical predictions for both cases, neutral hydrogen gas and hydrogen plasma as well [19,20].

In Fig. 2 we present the energy loss data for helium ions in the plasma during the discharge. At time zero, the gas volume is not ionized and the data show the energy loss of about 28 keV in the cold hydrogen gas at 1.94 mbar, which agrees with stopping-power calculations based on SRIM calculations [21]. Then the energy loss follows the increasing free electron density in the discharge region.

From Fig. 2 it is obvious that our measured energy loss (EXP, red diamond) exceeds the prediction of semiclassical approaches ( $Z_{\text{eff}}$ , blue) at the maximum by more than 30%, where the value of the effective charge is  $Z_{\text{eff}} = 1.43$ , according to the empirical formula of Ref. [22]. Solving the rate equations (RE) with all main excited states of the projectile for all relevant atomic processes our calculations (RE\_A, red) are in excellent agreement with the

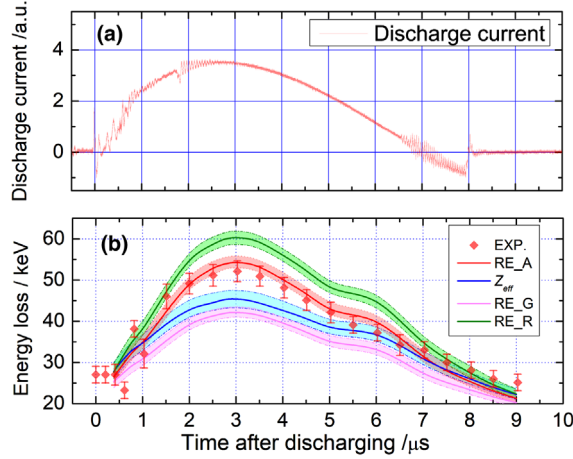


FIG. 2. Temporal evolution of discharging-current (a) and energy loss (b) of 100 keV He ion in the plasma. The green, red, blue, and pink regions stand for the predicted energy loss by models that radiation decays are excluded (RE\_R), all the main atomic states and atomic processes are included (RE\_A), the semiclassical calculation with effective charge ( $Z_{\text{eff}}$ ) and only ground states are included (RE\_G).

experimental data. In order to show the important influence of the excited states, and subsequent radiative decay for the stopping process, we also performed calculations where only ground state configurations were included (RE\_G, pink), and in another case we suppressed radiative decay (RE\_R, green). The uncertainties of the theoretical calculations arise from the uncertainty of the electron density of the target.

Since nuclear stopping is neglected, stopping of 100 keV/u helium ion in hydrogen plasma is mainly due to collisions with bound electrons ( $S_b$ ) and with free electrons ( $S_f$ ). In our model,  $S_b$  is calculated by classical trajectory Monte Carlo method [23,24] in an *ab initio* and self-consistent way. These calculations agree well with the experimental data [25] and theoretical predictions [26].  $S_f$  is calculated by dielectric-response theory [27]:

$$S_f = \frac{e^2}{\pi v_p^2} \int_0^\infty \frac{dk}{k} |Z_p - \rho(k)|^2 \int_{-kv_p}^{kv_p} d\omega \omega \text{Im} \left[ -\frac{1}{\varepsilon(k, \omega)} \right], \quad (1)$$

where  $\varepsilon(k, \omega)$  is the quantum dielectric function at plasmas [28],  $Z_p$  is the projectile nuclear charge, and  $\rho(k)$  is the Fourier transform of the projectile bound electron density, which in turn is depending on the electronic configuration of the projectile. The stopping power is then obtained by summing over both  $S_b$  and  $S_f$  for all the projectile atomic states:

$$S = \sum_i P(i) S(i) = \sum_i [P(i) S_b(i) n_b + P(i) S_f(i) n_f], \quad (2)$$

where  $P(i)$  denotes the fraction of the projectiles in atomic state  $i$ ,  $n_b$ , and  $n_e$  are the density of bound electron and free

electron, respectively. In our calculation, the ion trajectory is divided into infinitesimal parts. The atomic fractions are first calculated in one part and then based on this, the ion stopping is calculated in this part. Step by step, the total ion energy loss in plasma is obtained as

$$\Delta E = \int S dx. \quad (3)$$

Other than the effective charge approach ( $Z_{\text{eff}}$ ) of semiclassical theory, we take into account all relevant electronic configurations of the projectile, in addition all ionization and capture processes, such as charge transfer, impact ionization and excitation, and the respective reverse processes radiative decay (RD), radiative recombination. The dielectronic recombination (DR) and three-body recombination (3BR) are also included even though their contribution is very small given our plasma conditions [29,30]. We incorporated these processes by solving the rate equations during the slowing down process:

$$\frac{dP_i(v_p, t)}{dt} = \sum_{j \neq i} [\alpha(j \rightarrow i) P_j(v_p, t) - \alpha(i \rightarrow j) P_i(v_p, t)], \quad (4)$$

where  $P_i(v_p, t)$  denotes the time ( $t$ ) dependent fraction of the projectiles in configuration  $i$ , which in turn depends on the projectile velocity  $v_p$ ,  $\alpha(j \rightarrow i)$  is the rate coefficient for transitions from the configuration  $j$  to  $i$ . This is calculated by  $\alpha(j \rightarrow i) = v_p n_f \sigma(j \rightarrow i)$ , with the respective cross sections  $\sigma$  and ion velocity  $v_p$  or by direct calculation as radiative-decay rates. The cross sections for collisions of the projectiles with free electrons, bound electrons, and protons are calculated by solving the time dependent Schrödinger equation [31] or using the flexible atomic code of Ref. [32], or from data of Refs. [33,34].

In order to show the influence of the projectile excited states on its stopping, our calculation includes the excited states, step by step, till the principle number  $n = 10$ . Figure 3 points out that the model predicts an increase in energy loss when more excited states are included. Including only the ground state  $n = 1$  results in a predicted energy loss of 42 keV which is significantly lower than the experimental value of 52 keV. Our simulation indicates that beyond  $n = 4$  the increase levels off. Nevertheless, our calculation considers principal quantum numbers up to  $n = 10$ . A variation of  $n$  from  $n = 4$  up to  $n = 10$  increases the calculated energy loss value from 54.1 to 54.2 keV only, since highly excited states ( $n > 4$ ) are more easily ionized, even by collisions with large impact parameter. Therefore, the corresponding occupation number is much smaller than that with  $n4$ .

Figure 4 shows the atomic state distribution (a) and charge state distribution (b) of 100 keV/u helium ion in the plasma at the peak discharging time, when the free electron density reaches the maximum and the plasma is most

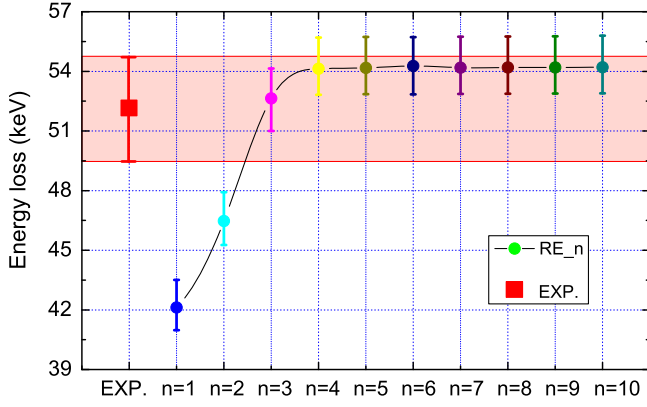


FIG. 3. Comparison of the measured energy loss with the calculated energy loss by solving the rate equation including the projectile excited states up to the principal quantum number  $n = 10$ .

stable. The atomic state distribution is calculated by RE which includes all relevant atomic states and related atomic processes (RE\_A). The corresponding charge state distribution for  $\text{He}^+$  and  $\text{He}$  is the sum over all their corresponding states. From Fig. 4(a) we conclude that,  $\text{He}^{2+}$  and the ground state of  $\text{He}^+$ , i.e.,  $1s$  state, are the dominant atomic states, while the total fraction of all the other excited states is less than 10%. However, if we do not include the excited state in the calculation [see Fig. 4(b) RE\_G], the charge state distribution will change significantly. It is interesting to note that our RE\_A calculation suggests a mean charge state of 1.44, which is very close to the effective charge state (1.43) deduced from the empirical formula in Ref. [22], but the effective charge description leads to a much lower energy-loss prediction (Fig. 3). If all the projectile electrons are assumed to be in the ground states, the RE\_G model predicts a much smaller effective

charge of 1.17, which fails to explain the energy loss as well. If radiative decay is artificially suppressed (RE\_R) in the model, it will lead to a remarkable increase of the mean charge state and an unacceptable overestimation of the energy loss. Therefore, it is concluded that the projectile excited states play an important role in ion stopping process, even though the population fraction of all excited states is only less than 10%.

Our calculation demonstrates that excited states are active to adjust the atomic state distribution, since the rate coefficient for the excited states can be much higher than that for the ground state. For instance, the electron capture cross section for a  $\text{He}^{2+}$  ion is much higher than that to its ground state, the radiative decay of excited  $\text{He}^+$  contributes most to the population of the ground state of  $\text{He}^+$  due to the high value of the rate coefficient. The impact ionization of the excited states of  $\text{He}^+$  is comparable to that of the ground state due to their lower ionization energy, and the collisional excitation processes are also key transfer channels, where the existence of excited states is necessary as well.

In summary, the stopping of low energy alpha particle in a hydrogen plasma was investigated both experimentally and theoretically [35]. By combining a high-performance accelerator in the 100 keV/ $u$  regime with a well-characterized homogenous plasma, valuable experimental data with high precision have been obtained. The measured energy loss exceeds the prediction of the commonly used semiclassical models by about 20%. This underpins the failure of the effective charge concept. Taking into account all relevant excited states of the projectile, and all main atomic processes, our model based on the rate equation excellently agrees with the measurements. We show that the active involvement of excited states in the charge transfer processes has a remarkable influence on the atomic state evolution and the stopping of the low energy ions in plasma. The experimental data and the theoretical methods provide an important support for the relevant research like DT-alpha heating and atomic process in solar wind.

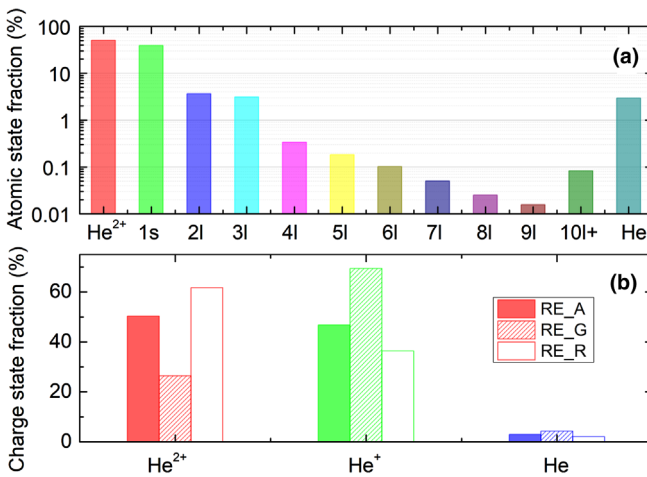


FIG. 4. Atomic state (a) and charge state (b) distributions for the hellion ion in plasma. RE\_A and RE\_G are the same as those in Fig. 3.

We sincerely thank the Jinyu Li and his co-workers for running the HIRFL accelerator. This work was supported by the National Key R & D Program of China (Grants No. 2017YFA0402300, No. 2017YFA0403200, and No. 2019YFA0404900), the Chinese Science Challenge Project No. TZ2016005, the NSAF (Grant No. U2030104), the National Natural Science Foundation of China (Grants No. U1532263, No. 11975174, No. 11574034, No. 11705141, No. 11775282, and No. U1530142), and the State Key Laboratory Foundation of Laser Interaction with Matter (Grant No. SKLLIM1807).

\*zhaoyongtao@mail.xjtu.edu.cn

†chengrui@impcas.ac.cn

‡hebin-rc@163.com



- [1] J. Ren, Z. Deng, W. Qi, B. Chen, B. Ma, X. Wang, S. Yin, J. Feng, W. Liu, Z. Xu *et al.*, *Nat. Commun.* **11**, 5157 (2020).
- [2] R. Betti and O. Hurricane, *Nat. Phys.* **12**, 435 (2016).
- [3] E. I. Moses, *Nucl. Fusion* **49**, 104022 (2009).
- [4] M. Basko, M. Churazov, and A. Aksenov, *Laser Part. Beams* **20**, 411 (2002).
- [5] W. Cayzac, A. Frank, A. Ortner, V. Bagnoud, M. Basko, S. Bedacht, C. Bläser, A. Blažević, S. Busold, O. Deppert *et al.*, *Nat. Commun.* **8**, 15693 (2017).
- [6] B. Y. Sharkov, D. H. Hoffmann, A. A. Golubev, and Y. Zhao, *Matter Radiat. Extremes* **1**, 28 (2016).
- [7] A. Frank, A. Blažević, V. Bagnoud, M. M. Basko, M. Börner, W. Cayzac, D. Kraus, T. Heßling, D. H. H. Hoffmann, A. Ortner *et al.*, *Phys. Rev. Lett.* **110**, 115001 (2013).
- [8] G. Belyaev, M. Basko, A. Cherkasov, A. Golubev, A. Fertman, I. Roudskoy, S. Savin, B. Sharkov, V. Turtikov, A. Arzumanov *et al.*, *Phys. Rev. E* **53**, 2701 (1996).
- [9] J. Jacoby, D. H. H. Hoffmann, W. Laux, R. W. Müller, H. Wahl, K. Weyrich, E. Boggasch, B. Heimrich, C. Stöckl, H. Wetzler *et al.*, *Phys. Rev. Lett.* **74**, 1550 (1995).
- [10] C. Deutsch and G. Maynard, *Matter Radiat. Extremes* **1**, 277 (2016).
- [11] L. C. Northcliffe, *Phys. Rev.* **120**, 1744 (1960).
- [12] P. Sigmund and A. Schinner, *Nucl. Instrum. Methods Phys. Res., Sect. B* **174**, 535 (2001).
- [13] N. Bohr and J. Lindhard, *Kgl. Danske Videnskab. Selsk. Mat.-Fys. Medd.* **28** (1954), <http://gymarkiv.sdu.dk/MFM/kdvs/mfm%2020-29/mfm-28-7.pdf>.
- [14] C. D. Boley, R. K. Janev, and D. E. Post, *Phys. Rev. Lett.* **52**, 534 (1984).
- [15] G. Xu, M. D. Barriga-Carrasco, A. Blažević, B. Borovkov, D. Casas, K. Cistakov, R. Gavrilin, M. Iberler, J. Jacoby, G. Loisch *et al.*, *Phys. Rev. Lett.* **119**, 204801 (2017).
- [16] D. H. H. Hoffmann, K. Weyrich, H. Wahl, D. Gardés, R. Bimbot, and C. Fleurier, *Phys. Rev. A* **42**, 2313 (1990).
- [17] A. Golubev, M. Basko, A. Fertman, A. Kozodaev, N. Mesheryakov, B. Sharkov, A. Vishnevskiy, V. Fortov, M. Kulish, V. Gryaznov *et al.*, *Phys. Rev. E* **57**, 3363 (1998).
- [18] A. Kuznetsov, O. Byalkovskii, R. Gavrilin, A. Golubev, K. Gubskii, I. Rudskoi, S. Savin, V. Turtikov, and A. Khudomyasov, *Plasma Phys. Rep.* **39**, 248 (2013).
- [19] R. Cheng, X. Zhou, Y. Wang, Y. Lei, Y. Chen, X. Ma, G. Xiao, Y. Zhao, J. Ren, D. Huo *et al.*, *Laser Part. Beams* **36**, 98 (2018).
- [20] Y.-H. Chen, R. Cheng, M. Zhang, X.-M. Zhou, Y.-T. Zhao, Y.-Y. Wang, Y. Lei, P.-P. Ma, Z. Wang, J.-R. Ren *et al.*, *Acta Phys. Sin.* **67**, 044101 (2018).
- [21] J. F. Ziegler, M. D. Ziegler, and J. P. Biersack, *Nucl. Instrum. Methods Phys. Res.* **268**, 1818 (2010).
- [22] S. Y. Guskov, N. Zmitrenko, D. Ilin, A. Levkovskii, V. Rozanov, and V. Sherman, *Plasma Phys. Rep.* **35**, 709 (2009).
- [23] R. E. Olson and A. Salop, *Phys. Rev. A* **16**, 531 (1977).
- [24] B. He, J. G. Wang, and R. K. Janev, *Phys. Rev. A* **79**, 012706 (2009).
- [25] S. K. Allison, *Rev. Mod. Phys.* **30**, 1137 (1958).
- [26] J. Ziegler, *J. Appl. Phys.* **85**, 1249 (1999).
- [27] W. Brandt and M. Kitagawa, *Phys. Rev. B* **25**, 5631 (1982).
- [28] S. Skupsky, *Phys. Rev. A* **16**, 727 (1977).
- [29] T. Peter and J. Meyer-ter Vehn, *Phys. Rev. A* **43**, 2015 (1991).
- [30] R. R. Haar, J. A. Tanis, V. L. Plano, K. E. Zaharakis, W. G. Graham, J. R. Mowat, T. Ellison, W. W. Jacobs, and T. Rinckel, *Phys. Rev. A* **47**, R3472 (1993).
- [31] C. L. Liu, S. Y. Zou, B. He, and J. G. Wang, *Chin. Phys. B* **24**, 093402 (2015).
- [32] M. F. Gu, *Can. J. Phys.* **86**, 675 (2008).
- [33] R. R. Haar, J. A. Tanis, V. L. Plano, K. E. Zaharakis, W. G. Graham, J. R. Mowat, T. Ellison, W. W. Jacobs, and T. Rinckel, *Phys. Rev. A* **47**, R3472 (1993).
- [34] T. G. Winter, *Phys. Rev. A* **76**, 062702 (2007).
- [35] See Supplemental Material at <http://link.aps.org/supplemental/10.1103/PhysRevLett.126.115001> for more details.